ELSEVIER

Journal of Organometallic Chemistry 515 (1996) 183–191

Journal of Organometallic Chemistry

Inter- vs. intramolecular rearrangement of a $(Bu_3P)_2Ni$ moiety in its 9-alkyl and 9,10-dialkyl anthracene complexes. Limiting conditions and isomer stabilities

Amnon Stanger *, Haim Weismann

Department of Chemistry, Technion-Israel Institute of Technology, Haifa 32000, Israel

Received 17 October 1995

Abstract

The $(Bu_3P)_2Ni$ complexes of 9-alkyl and 9,10-dialkylanthracene (alkyl = Me, Et) were prepared and their structural and dynamic properties studied. It was found that in the 9-substituted systems the nickel is bound η^2 to C(3)–C(4) of the anthracene. Based on chemical shift analysis of similar systems [e.g. $(Bu_3P)_2Ni$–anthracene and (depe)Ni–anthracene] and spin saturation transfer experiments, it was determined that the 9,10-dialkyl anthracenes are not η^4 complexes (as appears from the NMR spectra) but η^2 complexes in which two isomeric (however, chemically identical) structures equilibriate rapidly.

The dynamic behavior of the systems was studied using spin saturation transfer and line shape analysis VT-NMR techniques. It was found that in all the systems under study the $(Bu_3P)_2Ni$ moiety rearranges between the two terminal rings of the anthracene. In the 9-substituted systems (**3**) there are two rearrangement pathways: an intramolecular one (with $\Delta H^{\ddagger}$ of ca. 8 kcal mol^{-1} and a negative $\Delta S^{\ddagger}$) and an intermolecular rearrangement with $\Delta H^{\ddagger}$ of ca. 20 kcal mol^{-1} and a positive $\Delta S^{\ddagger}$. The 9,10 disubstituted anthracene complexes (**4**) show two intermolecular rearrangements, each of them with similar activation parameters as the intra- and intermolecular rearrangements of **3**. All the rearrangements are of a kinetic first order. On the basis of these data a rearrangement mechanism is proposed.

Using magnetization transfer to a hidden partner it was found that a methyl destabilises the Ni–anthracene bond by 1.2–3 kcal mol^{-1}, probably because of steric effects.

Keywords: Nickel; 9,10-dialkyl anthracene; Dynamic behavior; Fluxionality; Kinetics; Nuclear magnetic resonance

1. Introduction

Dynamic processes in organometallic complexes are relatively common [1]. Of particular interest are those that, when quantitatively measured, can supply physical data that could eventually lead to rational design of catalysts and reaction mediators. As nickel based complexes are of the more popular catalysts used for organic syntheses in academic research [2], as well as in industry [3], it is our goal to obtain "physical organometallic" parameters for $(R_3P)_2Ni(0)$ moieties. A "parent system" (**1**) was defined and thoroughly investigated. In the solid state the coordination between the Ni and anthracene is η^2 [4]. In solution, the proton NMR spectra show AA'BB' patterns, which indicate η^4 coordination, but may also result from fast equilibriation ($\Delta G^{\ddagger} \leq 4$ kcal mol^{-1}) [5] between two η^2 structures, similar to that observed for analogous naphthalene complexes [6]. An intramolecular rearrangement [7] of the $(Bu_3P)_2Ni$ moiety between the two terminal rings of the anthracene is also observed [5]. Alternations in the system (even minor ones) cause sometimes dramatic changes in some of these properties. For example, when (depe)Ni (**2**) is used instead of $(R_3P)_2Ni$ (R = Bu, Et) the complex is a mixture of η^3 and η^4 isomers in the solid state (below -10°C) [8]. The (depe)Ni moiety in **2** undergoes an intermolecular rearrangement between the terminal rings, with a much smaller activation energy [8]. The effect of fine changes in the arene is not clear as yet, and thus we decided to investigate the effect of mild substitutions — methyl and ethyl — at a distant position from the coordination site (the 9,10 positions of the anthracene) on the structures and dynamic processes of the systems.

* Corresponding author.

SSDI 0022-328X(95)06104-5

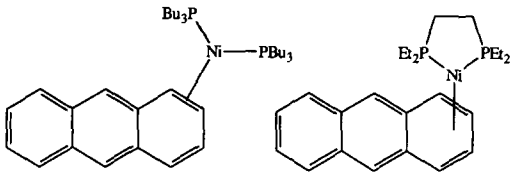

1 2

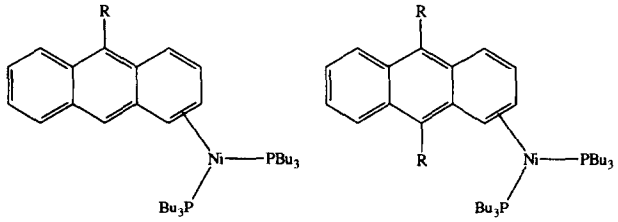

3 a: R=Me
b: R=Et

4 a: R=Me
b: R=Et

To that purpose we have prepared **3** and **4**. The compounds were prepared using literature procedures [9]. All the structural and kinetic studies were carried out in THF-d_8 solution, using VT-NMR, spin saturation transfer (SST) and line shape analysis (LSA) methods.

2. Results and discussion

2.1. Structure

All the L_2Ni complexes of anthracenes that have a C_2 symmetry element around the long axis of the ligand show (at a temperature lower than coalescence [5]) two AA'BB' patterns, one at a higher field (H_1–H_4) and the second at a lower field (H_5–H_8) [5]. This indicates either η^4 binding between the Ni and the anthracene or fast equilibriation between two η^2 structures. Cooling the samples to ca. −100°C does not change the spectra, and thus a maximum barrier of 4 kcal mol^{-1} was assigned to the $\eta^2 \rightleftarrows \eta^2$ process (if it exists) [5]. The solid state structure of **1** (and also of the Et_3P derivative) clearly shows that the Ni is bound η^2 to the

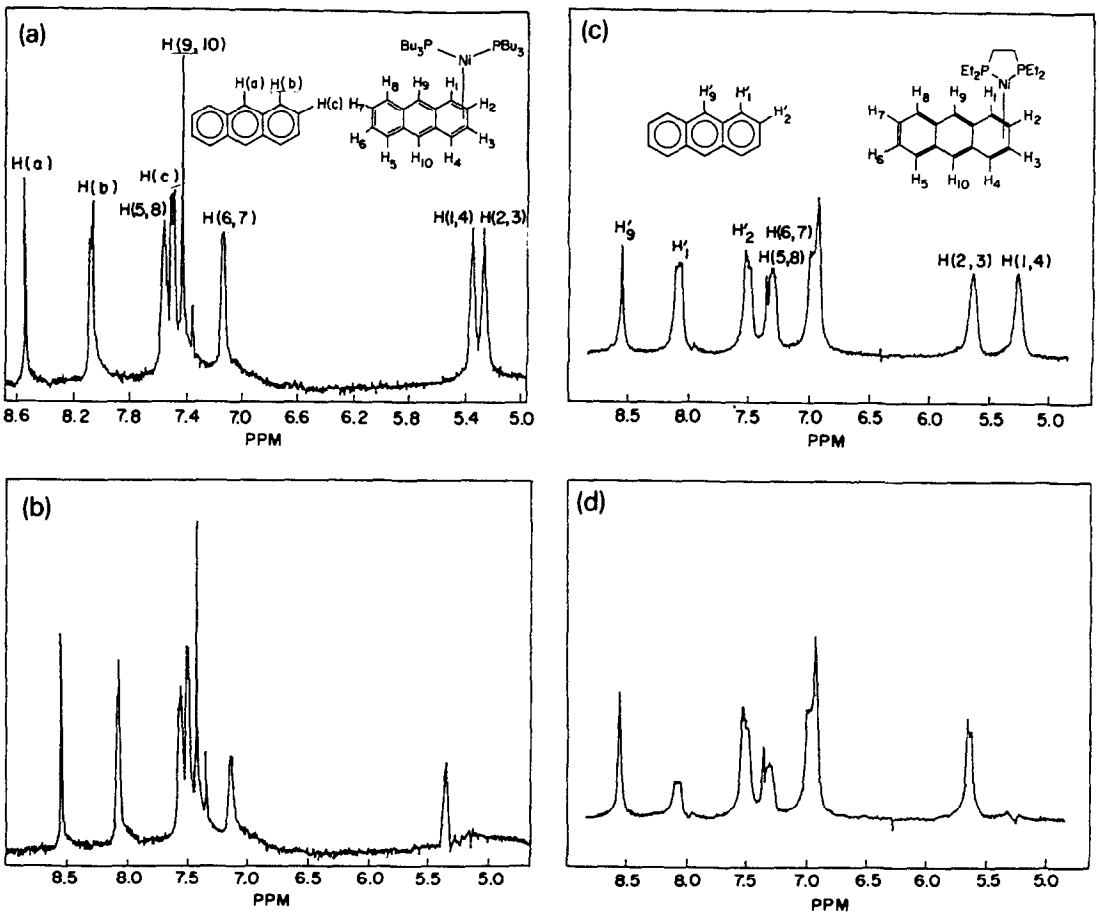

Fig. 1. Saturation transfer experiments with **1** and **2** in the presence of free anthracene. (a) The anthracene region of **1**; (b) the same as (a) with saturation of the right part of the high field AA'BB'; (c) the anthracene region of **3**; (d) the same as (c) with saturation of the right part of the high field AA'BB'.

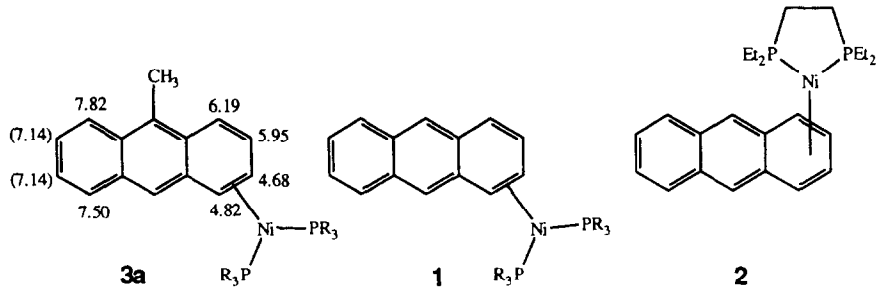

H	(AV)		
2,3	5.32	5.27	5.65
1,4	5.51	5.34	5.23
6,7	7.14	7.15	6.98
5,8	7.66	7.55	7.30

Scheme 1. Chemical shifts of **1**, **2** and **3a**.

anthracene in both complexes [4]. None the less, the structures show solid state interactions that stabilize the η^2 structures relative to the alternative η^4 complexes [4], and thus it is unclear which is the stable structure in solution. We present here an NMR based technique for the determination of the stable coordination without freezing the dynamic process, if it exists.

When H(2, 3) of **1** (the right peak of the high field AA'BB') are saturated, the magnetization is transferred to H(6, 7) of the complex (the right peak of the low field AA'BB') only, and the free ligand signals do not change (Figs. 1(a) and 1(b)) [7]. When the same experiment is carried out on **2** (which is η^3 and η^4 in the solid state [8]) two major differences (relative to **1**) can be observed (Figs. 1(c) and 1(d)). One is that the saturation is transferred to the free ligand as well as to the other side of the complex, and the other is that when the right peak of the high field AA'BB' is saturated the magnetization is transferred to the left parts of the low field AA'BB' and of the free ligand. The magnetization transfer to the free ligand means that there is an intermolecular rearrangement of the (depe)Ni moiety [7] (possibly also intramolecular), but how can the change in the "right to right" vs. "right to left" saturation transfer be accounted for?

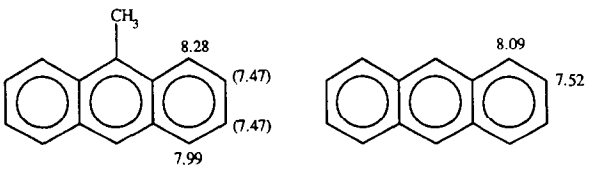

Fig. 2. Chemical shifts of 9-methyl anthracene and anthracene.

The complexes which are non-symmetric with respect to the above mentioned C_2 axis of the anthracene (for example **3**) are η^2 complexes, where the Ni is bound to C(3) and C(4). If these complexes were fast equilibriating, the signals of H(1) and H(2) would average with those of H(4) and H(3) respectively. Since the effect of a 9-methyl substitution at the anthracene on the chemical shifts of H(1)–H(4) is not larger than 0.05 ppm (Fig. 2) [10], one can calculate the average chemical shifts of fast equilibriating η^2 structures of **3a** (within ± 0.05 ppm). This is presented in Scheme 1, together with the chemical shifts of **1** and **2**.

The calculated average chemical shifts of **3a** are very similar to these observed for **1** and different from these of **2**. This is especially true for the low/high field issue; whereas in fast equilibriating η^2 structures H(1, 4) resonate at lower field than H(2, 3), the opposite is true for an η^4 complex (**2**). We therefore conclude that η^2 complexes that are fast equilibriating show "right to right" (or "left to left") magnetization transfer (regarding the two AA'BB' patterns), whereas η^4 complexes show "right to left" (or "left to right") saturation transfer.

Another support to this analysis comes from the ^{31}P spectra; Scheme 2 shows a schematic top view of the two complexes. The chemical shift difference between the two phosphines of an η^2 complex results from a simple chemical environment difference, whereas in an η^4 complex the difference should be larger due to the

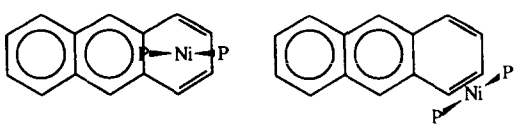

Scheme 2. Schematic top view of an η^4 complex (left) and an η^2 complex (right).

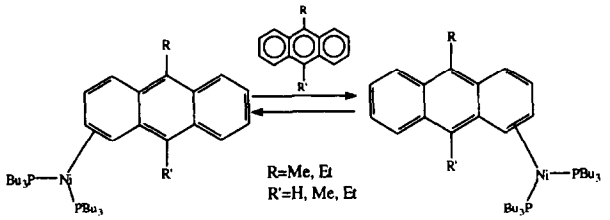

Fig. 3. The haptotropic rearrangements studied for **3** and **4**.

ring current of the naphthalenic residue. Indeed, in most $(Bu_3P)_2Ni$–anthracene complexes the chemical shift difference between the phosphines is 8–12 ppm. In **2** the respective difference is 29 ppm.

To conclude, the chemical shift analysis and the saturation transfer experiments described above enable the determination of the stable coordination number of the complexes under investigation very easily; all that is required is to measure an NMR spectrum at a temperature under which saturation transfer can be observed. According to the signals that are paired by saturation transfer (i.e. "right-to-right" or "right-to-left") one could tell if the complex under study is a "real" η^4 complex or is actually an η^2 structure under fast equilibriation. Using this technique it was found that **4a** and **4b** are η^2 complexes.

2.2. Kinetics

The molecularity of the processes (Fig. 3) was determined using spin saturation transfer techniques [7]. It was found that for all the compounds magnetization is transferred to the respective free ligand as well as to the other side of the coordinated ligand. This indicates an intermolecular rearrangement, but does not rule out the existence of an intramolecular process. The reaction, however, is of first order, i.e. the rearrangement rates are not sensitive to the concentrations and to the complex/free ligand ratio (1 : 0.7 to 1 : 10 in different experiments). Thus, although the reaction involves a migration of $(Bu_3P)_2Ni$ from one anthracene ligand to another, the rate determining step is unimolecular, and depends only on the complex. Table 1 lists the measured rates as a function of temperature, and Fig. 4

Table 1
Temperatures and rate constants for the different processes in **3a**

T	k_{intra}	T	k_{inter}	T	k_{coal} [a]
249.4	$(6.95 \pm 2.88) \times 10^{-2}$	231.5	0.665 ± 0.034	281.9	24
258.4	0.254 ± 0.092	240.4	1.33 ± 0.53	287.8	66
267.4	1.26 ± 0.39	249.4	2.00 ± 0.54	299.2	314
276.2	5.38 ± 0.25	258.4	4.28 ± 0.59	305.3	520
281.7	10.27 ± 0.34	267.4	6.47 ± 1.08	312.5	1000
288.2	20.81 ± 2.60				

[a] The error in the rates obtained from line shape analysis is estimated to be ca. ±25%.

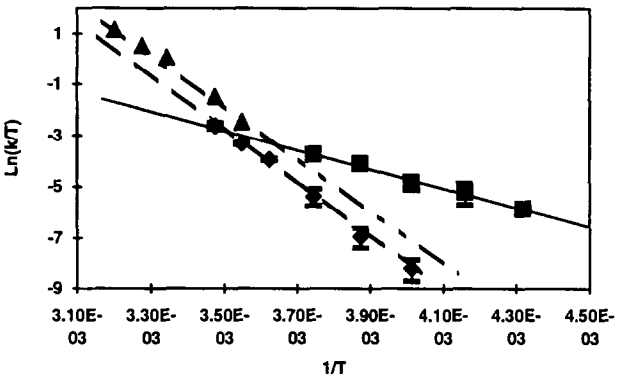

Fig. 4. Eyring plots of the dynamic processes in **3a**. ■, Formal intramolecular process (magnetization transfer to the respective site at the complex); ♦, formal intermolecular process (magnetization transfer to the respective site at the free ligand); ▲, data from ^{31}P line shape analysis.

shows the Eyring plot of the processes (described in Fig. 3) for **3a**. There is a line formed from the data of each of the kinetic probes; the intra- and intermolecular SST (formal intra- and intermolecular rearrangements respectively), and the third for the coalescence process of the ^{31}P spectra. Table 2 lists the activation parameters for the process: the intramolecular process has an activation enthalpy of 7.3 kcal mol^{-1} and a large negative entropy of activation. The intermolecular SST and the ^{31}P coalescence processes have the same activation parameters (within experimental error) and involve a much higher activation enthalpy and a positive entropy of activation. The ethyl derivative (**3b**) has been studied for comparison, and shows the same kinetic features. The formal intramolecular process [11] has a $\Delta H^{\ddagger}$ of 7.7 ± 0.46 kcal mol^{-1} and a large negative $\Delta S^{\ddagger}$ (-26.5 ± 2.7 e.u.). The free energies of activation for the intermolecular and ^{31}P coalescence processes for **3a** and **3b** are summarized in Table 3.

Table 2
Reaction parameters of the rearrangements of **3a** (see Fig. 4 for definition of the symbols)

	$\Delta H^{\ddagger}$ (kcal mol^{-1})	$\Delta S^{\ddagger}$ (e.u.)	Correlation
■	7.3 ± 0.4	-26.5 ± 2.7	0.9919
♦	20.9 ± 0.6	20.9 ± 2.2	0.9984
▲	19.7 ± 1.1	18.7 ± 3.5	0.9942

Table 3
Free energies of activation for the dynamic processes in **3a** and **3b** (symbols as in Table 2)

	$\Delta G^{\ddagger}$ (290 K)	$\Delta G^{\ddagger}$ (345 K)
3a ♦	14.8 ± 1.2	13.7 ± 1.4
3a ▲	14.3 ± 2.2	13.3 ± 2.3
3b ♦	13.8 ± 2.0	13.7 ± 2.2
3b ▲	14.0 ± 2.6	13.6 ± 2.8

Table 4
Temperatures and rate constants for the different processes in **4a**

T	k_{intra}	T	k_{inter}	T	k_{coal} [a]
250.6	0.142±0.011	255.1	0.488±0.268	263.8	5
261.1	0.401±0.081	263.9	0.828±0.293	301.0	725
271.7	0.438±0.090	273.2	2.75 ±0.96	307.9	1450
281.7	0.916±0.201	281.7	2.69 ±0.81	312.2	1825
296.7	3.40 ±1.01	295.0	5.54 ±2.14	316.7	2800

[a] The error in the rates obtained from line shape analysis is estimated to be ca. ±25%.

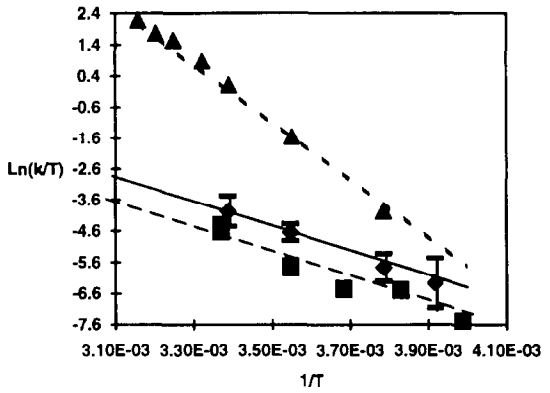

Fig. 5. Eyring plots of the dynamic processes in **4a**. Definition of symbols as in Fig. 4.

Table 5
Activation parameters for the dynamic processes in **4a** (symbols as in Table 2)

	$\Delta H^{\ddagger}$ (kcal mol^{-1})	$\Delta S^{\ddagger}$ (e.u.)	Correlation
■	8.8±1.3	−26.3±4.8	0.969
◆	8.6±0.2	−25.5±0.7	0.999
▲	19.5±0.5	19.1±1.6	0.999

The free energies of activation indicate that both **3a** and **3b** undergo the same processes, with virtually the same activation energies. Thus, two processes are observed; one is an intramolecular rearrangement of the $(Bu_3P)_2Ni$ moiety between the two terminal rings of the anthracene, and an intermolecular process that is manifested by intermolecular SST and coalescence of the ^{31}P signals. It therefore appears that the alkyl substitution at the 9 position of the anthracene has opened a second (intermolecular) rearrangement path, which is not observed in **1**.

The effect of a double methyl substitution (at the 9 and 10 positions of the anthracene) was determined from the kinetic studies of **4a**. Table 4 lists the temperature dependent rates, and Fig. 5 and Table 5 show the Eyring plots and the activation parameters respectively of the measured dynamic processes (Fig. 3). As in **3a**, there are three lines formed, but here the (formal) intra- and intermolecular processes show the same activation parameters, which are similar to those of the intramolecular rearrangement in **3**. Thus, it is necessary to

Table 6
Free energies of activation of **4a** and **4b** (symbols as in Table 2)

		290 K	345 K
4a	■	16.4±2.7	17.9±3.0
	◆	16.0±0.4	17.4±0.9
	▲	14.0±1.0	12.9±1.0
4b	■	16.0±0.8	16.7±0.8
	◆	15.8±1.1	16.7±1.2
	▲	13.6±2.4	12.9±2.6

conclude that there is only one process which is intermolecular that is monitored by SST, and has (probably) the same rate determining transition state as the intramolecular process in **3**. The process manifested by the coalescence of the ^{31}P signals has the same activation parameters as the respective process in **3**, and is thus assumed to have the same mechanism. The ethyl derivative (**4b**) shows essentially the same behavior, as can be learned from the activation parameters listed in Table 6.

Based on the kinetic studies outlined above, a mechanism was postulated and its qualitative energy profile is described in Fig. 6. We suggest that there are two operating mechanisms for rearrangements in these systems [12]. The first one is a movement of the $(Bu_3P)_2Ni$ moiety (from the starting material. (SM)) along the π system towards the central ring of the anthracene, with $\Delta H^{\ddagger}$ of 7–8 kcal mol^{-1} and a negative $\Delta S^{\ddagger}$ [13], leading (probably through a coordination change and incorporation of a solvent molecule as a ligand) to a high energy intermediate (**A**) [14]. As this step is rate determining, the following (fast) processes do not affect the rates of the processes. The intermediate **A** further reacts via two possible pathways: one is a "jump" of the $(Bu_3P)_2Ni$ fragment across C(9) to form the symmetric intermediate **A'** (e.g. as in **1** and **3**), which proceeds to the intramolecular rearranged product. However, in case of substitution (such as an alkyl that causes steric hindrance) the barrier for this "jump" increases. In these cases (e.g. **4**), another direction of the reaction operates, namely the dissociation of **A** to solvated $(Bu_3P)_2Ni$ and free arene (**B**) [14]. The

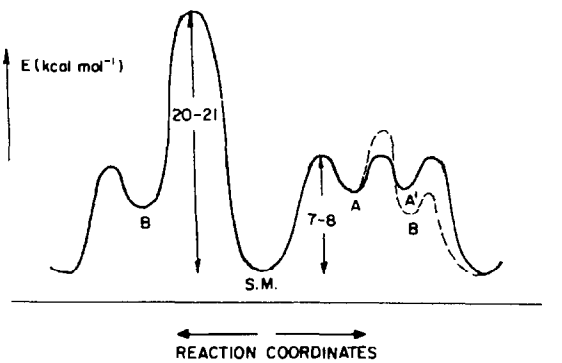

Fig. 6. Schematic energy profile of the rearrangements in **3** and **4**.

$(Bu_3P)_2Ni$ moiety recombines either to an initially free ligand, which is manifested by the intermolecular saturation transfer, or to the initially coordinated ligand (which is manifested by the formal intramolecular rearrangement). Note that an intermolecular process of this type is not observed in **3**, but in **4** only. Thus, the effect of alkyl substitution at this transition state is at least 3 kcal mol^{-1}. This is in accordance with other findings regarding the effect of a methyl at the 9 position of the anthracene (see below).

The high energy intermolecular pathway observed in **3** and **4** probably occurs via a different pathway (for example sliding of the metal directly outside) that leads to direct dissociation [14] and has a large positive $\Delta S^{\ddagger}$. Clearly, the coalescence of the phosphines does not result from rotation around the Ni–arene bond [15]. This (direct dissociation) pathway may occur also in **1** [16].

2.3. The thermodynamic effect of a methyl group at the 9 position of the anthracene on the Ni–arene bond

When the apparent H(3) of **3a** is saturated, a decrease of the signal attributed to H(2) is observed. This cannot be caused by a simple saturation transfer (i.e. magnetization transfer between protons that become equivalent due to homotopic reaction). NOE is also not the reason for this [17], and therefore we conclude that this is caused by magnetization transfer to a "hidden partner" [18]. Hence, although the signals of **3a′** are not observed (because of its low concentration and line broadening due to equilibrium with **3a**), the signal of H(2′) lies under the signal of H(3) [19]. When this is irradiated the saturation is transferred from H(2′) to H(2) due to the equilibrium **3a** ⇄ **3a′**. At the same time saturation is also transferred from H(3) to H(3′). However, since the signals of **3a′** are not observed, this saturation transfer has no effect on the observed spectra. This saturation transfer was studied as a function of temperature. The temperature dependent rates and the Eyring plot of the data are given in Table 7 and Fig. 7 respectively. The $\Delta H^{\ddagger}$ is ca. 7 kcal mol^{-1}, i.e., 3 kcal mol^{-1} higher than the maximum barrier assigned for the same respective process in the parent system **1**. In order to estimate the lower limit for this methyl effect, we have run spectral simulations for different ratios between **3a** and **3a′**. It turns out that when the ratio is 1:7 **3a′** could still (hardly, however) be observed. This implies that the $\Delta\Delta H_f$ [20] between the two isomers is at least 1.2 kcal mol^{-1}. Thus, **3a** is more stable than **3a′** by 1.2–3 kcal mol^{-1}. Assuming that **3a′** is geometrically relaxed while equilibriating, it is concluded that the 9-methyl substitution weakens the Ni–anthracene bond by 1.2–3 kcal mol^{-1}.

Table 7
Temperature dependent rates of the processes **3a** ⇄ **3a′**

T	k
232.3	0.177 ± 0.003
237.8	0.243 ± 0.036
250.4	0.542 ± 0.012
254.5	0.743 ± 0.175
262.9	1.05 ± 0.01
266.4	1.38 ± 0.07
270.4	1.71 ± 0.05

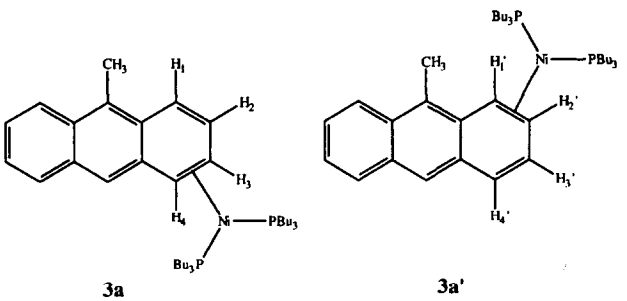

3a **3a′**

3. Summary and conclusions

The dynamic and structural properties of L_2Ni–arene complexes are extremely sensitive to small changes in the systems. In early investigations it was shown that the type of phosphine and the strong substitution at the arene change the coordination number and dynamics [8,21]. In this paper it is shown that even mild substituents, methyl and ethyl, have a considerable effect on these properties. A single alkyl substitution at the 9 position of the anthracene is enough to make one η^2 structure (**3a**) more stable than the second (**3a′**) by 1.2–3 kcal mol^{-1}. This single substitution allows an intramolecular rearrangement (as in the parent complex

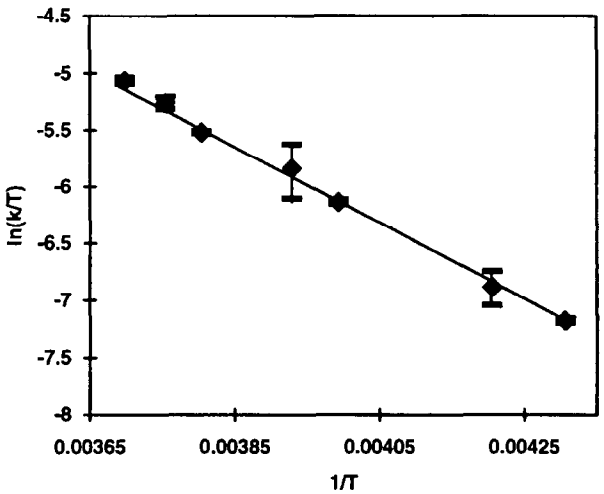

Fig. 7. Eyring plot of the rearrangement **3a** ⇄ **3a′**. $\Delta H^{\ddagger} = 6.9 \pm 0.2$ kcal mol^{-1}, $\Delta S^{\ddagger} = -3.1 \pm 0.6$ e.u., correlation 0.9987.

Table 8
^{1}H NMR spectra of **3a** (−23°C) and **3b** (−38°C)

	3a	3b
H(1)	6.20 (ps d)	6.33 (ps d)
H(2)	5.95 (m)	6.17 (m)
H(3)	4.68 (m)	4.50 (m)
H(4)	4.83 (m)	4.69 (m)
H(5)	7.52 (ps d)	7.60 (ps d)
H(6,7)	7.15 (m, 2H)	7.15 (m, 2H)
H(8)	7.52 (ps d)	7.85 (ps d)
H(10)	7.37 (s)	7.40 (s)
9-alkyl	2.52 (s, 3H)	3.10 (q, 2H, $^3J_{H-H}$ = 7.0) [a]
P[(*CH*$_2$)$_3$CH$_3$]$_3$	1.43, 1.13 (m, 36H)	1.41, 0.93 (two m, 57H, phosphines and 9-CH$_2$*CH*$_3$)
P[(CH$_2$)$_3$*CH*$_3$]$_3$	0.96, 0.84 (ps t, 18H)	

[a] The CH$_3$ resonance is buried under the phosphine signals.

1) and opens another intermolecular rearrangement channel, probably through direct dissociation. The doubly substituted systems (**4a** and **4b**) show two intramolecular rearrangements; one starts as the intramolecular rearrangement in **3**, but after the rate determining step the metallic fragment dissociates from the arene, and the other is a direct dissociation. We currently continue to investigate these systems in different solvents and with different substitutions.

4. Experimental section

The free ligands (9-alkylanthracene and 9,10-dialkylanthracene, alkyl = Me, Et) were prepared according to the procedure of Cho and Harvey [9a]. The (Bu$_3$P)$_2$Ni complexes were prepared according to our procedure [9b]. THF-d_8 was kept in a bomb on potassium benzophenone and vacuum transferred to the NMR tubes which were fire sealed. NMR spectra of the complexes were taken in THF-d_8. **3a**: ^{1}H (see Table 8). ^{13}C {^{1}H} (−23°C): 124.6, 124.4, 124.1, 124.0 [C(5)–C(8), broad unresolved signals], 109.6, 99.6 [C(1)–C(2)], 71.5 [C(3)–C(4), broad unresolved signals], 128 [C(10)], 140.4, 134.8, 134.0, 132.0 [C(9), C(11)–C(14) [22]], 15.6, 15.4, 15.2 [9-methyl and two P–(CH$_2$)$_3$–*CH*$_3$], 30–25 [P–*(CH*$_2$*)*$_3$–CH$_3$, partially buried under the solvent peaks]. ^{31}P {^{1}H} (−23°C): 12.5 (d), 1.9 (d) ($^2J_{P-P}$ = 51.6). **3b**: ^{1}H (see Table 8). ^{13}C {^{1}H} (−38°C): 124.6, 124.5, 124.0 [C(5)–C(8), broad unresolved signals], 116.4, 104.4 [C(1)–C(2)], 67–70 [C(3)–C(4), broad unresolved signals partially buried under solvent peaks], 128.5 [C(10)], 109.6, 99.6 [C(1)–C(2)], 71.5 [C(1)–C(2), broad unresolved signals], 148.7, 141.1, 138.1, 134.4, 133.7 [C(9), C(11)–C(14)], 30–25 [P–*(CH*$_2$*)*$_3$–*CH*$_3$, partially buried under the solvent peaks], 22.5 [9–*CH*$_2$CH$_3$], 15.64, 15.2 [P–(CH$_2$)$_3$–*CH*$_3$, and 9-CH$_2$*CH*$_3$]. ^{31}P {^{1}H} (−38°C): 13.1 (d), 4.0 (d) ($^2J_{P-P}$ = 52.0). **4a**: ^{1}H (see Table 9). ^{13}C {^{1}H} (−13°C): 125.1, 124.2 [C(5)–C(8)], 88.5, 84.3 [C(1)–C(4)], 136.4, 132.7, 120.9 [C(9)–C(14)], 15.2, 15.1, 15.0 [9,10-dimethyl and two P–(CH$_2$)$_3$–*CH*$_3$], 30–25 [P–*(CH*$_2$*)*$_3$–CH$_3$, partly buried under solvent peaks]. ^{31}P {^{1}H} (0°C): 16.1 (d), 1.38 (d) ($^2J_{P-P}$ = 49.9). **4b**: ^{1}H (see Table 9), ^{13}C {^{1}H} (−30°C): 124.8, 124.2 [C(5)–C(8)], 88.7, 82.4 [C(1)–C(4)], 136.6, 135.7, 127.7 [C(9)–C(14)], 22.7 [9,10-*CH*$_2$CH$_3$], 15.9, 15.4, 15.0 [9,10-CH$_2$*CH*$_3$ and two P–(CH$_2$)$_3$–*CH*$_3$], 30–25 [P–*(CH*$_2$*)*$_3$–CH$_3$, partly buried under solvent peaks]. ^{31}P {^{1}H} (−26°C): 17.1 (d), 2.48 (d) ($^2J_{P-P}$ = 48.8).

All the kinetic studies were carried out in fire-sealed NMR tubes to which the compounds were transferred under Ar and the solvent (THF-d_8) was vacuum transferred. A signal was saturated by CW selective irradiation at its resonance frequency. A spectrum was taken and the integrations (preset zeros) were measured for peaks at the respective sites of the complex and the free ligand (formal intra- and intermolecular rearrangements respectively) for each of these irradiations. In **4a** this was done for three peaks of the complex and three

Table 9
^{1}H NMR spectra of **4a** (25°C) and **4b** (−11°C)

	4a	4b
H(1,4)	5.58 (m)	5.68 (m)
H(2,3)	5.19 (m)	5.51 (m)
H(5,8)	7.67 (m)	7.81 (m)
H(6,7)	7.01 (m)	7.14 (m)
9,10-dialkyl	2.45 (s, 6H)	3.10 (q, 4H, $^3J_{H-H}$ = 7.2, *CH*$_2$CH$_3$) 1.22 (t, 6H, $^3J_{H-H}$ = 7.2, CH$_2$*CH*$_3$)
PBu$_3$	1.25, 0.81 (two m, 54H)	1.40, 0.92 (two m, 54H)

peaks of the free ligand, which yielded four probes of the intermolecular and three probes of the intramolecular magnetization transfers. In **3a** this was done for four peaks of the complex and three peaks of the free ligand, out of which the intramolecular magnetization transfer and intermolecular magnetization transfer were measured for two and seven probes respectively. At each temperature a "dummy" experiment (i.e. a spectrum measured with the CW irradiation at a "signal free" frequency) was carried out as a reference. This procedure was repeated three times at each temperature. T_{1effc}, was measured for each of the signals under saturation conditions of the signal with which it interchanges, by the inverse recovery method. The rates were calculated from the formula $k = (1/T_{1effc})[(M_{0A}/M_{\infty A}) - 1]$, where M_{0A} and $M_{\infty A}$ are the integrations under the dummy saturation and exchanging signal saturation respectively relative to a standard [23]. NOE effects were not found between any adjacent protons (at two extreme temperatures) and thus were not taken into account [17]. For each temperature there were three and two rates obtained for the formal intramolecular process for **4a** and **3a** respectively (for example, from the decrease of H(6, 7) and H(5, 8) under the saturation of H(2, 3) and H(1, 4) of **4a** respectively) and four and seven rates for the intermolecular processes in **4a** and **3a** respectively. Each of these were measured and calculated three times (as mentioned). Thus, at each temperature the rates that are used for the Eyring calculations are the average of 12 and 21 values for the formal intermolecular rearrangements in **4a** and **3a** respectively, and nine and six values for the formal intramolecular rearrangement in **4a** and **3a** respectively. The respective rates for **3b** and **4b** were obtained from about half the probes and at four temperatures for each of the processes (i.e. the formal intra- and intermolecular saturation transfer and coalescence of the ^{31}P lines). The temperatures were calibrated with external MeOH.

Acknowledgments

We thank Dr. Hugo Gottlieb (Bar Ilan University) for helpful discussions. Volkswagen Stiftung and The Israel Academy for Science and Humanities are acknowledged for financial support.

References and notes

[1] T.A. Albright, *Orbital Interaction in Chemistry*, Wiley Interscience, New York, 1985.
[2] G. Wilke, *Angew. Chem., Int. Ed. Engl., 27* (1988) 185.
[3] W. Keim, *Angew. Chem., Int. Ed. Engl., 29* (1990) 235.
[4] A. Stanger and R. Boese, *J. Organomet. Chem., 430* (1992) 235.
[5] A. Stanger and K.P.C. Vollhardt, *Organometallics, 11* (1992) 317.
[6] (a) R. Benn, R. Mynott, I. Topalović and F. Scott, *Organometallics, 8* (1989) 2299; (b) F. Scott, C. Krüger and P. Betz, *J. Organomet. Chem., 387* (1990) 113.
[7] A. Stanger, *Organometallics, 10* (1991) 2979.
[8] R. Boese, A. Stanger, P. Stellberg and A. Shazar, *Angew. Chem., 105* (1993) 1500; *Angew. Chem., Int. Ed. Engl., 32* (1993) 1475.
[9] (a) R.G. Harvey and H. Cho, *J. Am. Chem. Soc., 96* (1974) 2434; (b) A. Stanger and A. Shazar, *J. Organomet. Chem., 458* (1993) 233.
[10] The splitting pattern is different (AA'BB' for anthracene, ABCD for 9-methyl–anthracene). However, since an AA'BB' pattern can be regarded as an averaged ABCD, the average chemical shifts can be calculated.
[11] We call it here "formal intramolecular process" because it may arise from an intra- as well as from an intermolecular process (see the discussion regarding **4**). Thus, the data arrived from intramolecular saturation transfer, and is therefore named in this way.
[12] Two similar mechanisms were suggested for $(CO)_3Cr$–naphthalene on the basis of theoretical studies. See T.A. Albright, P. Hofmann, R. Hoffmann, C.P. Lillya and A. Dobosh, *J. Am. Chem. Soc., 105* (1983) 3396.
[13] It is well known that NMR is not a reliable method for the determination of $\Delta S^{\ddagger}$. However, the similarities between the values obtained for **3a** and **4a** and the comparison of the free energies of activation between **3a**, **3b** and **4a**, **4b** suggest that, at least in the bulk part, the values are correct. Thus, in the analysis presented one process is considered to have large negative $\Delta S^{\ddagger}$, and the other a positive value.
[14] This point is under investigation but the analysis is not simple owing to the two operating mechanisms that involve dissociation of the $(Bu_3P)_2Ni$ moiety, one at the rate determining step and the other after the rate determining step.
[15] There are two arguments to back this statement. One is that in **3** the coalescence of the phosphines has the same reaction parameters as the intermolecular SST, and the second is that the rotational barrier around L_2M(olefin) is much higher than the energies we measure here. For example, the rotational barrier of the $(Ph_3P)_2Pt$ moiety around the Pt–ethylene bond in $(Bu_3P)_2Pt$(ethylene) is 87.6 kcal mol^{-1}. For a summary see P.W. Jolly and G. Wilke, *The Organic Chemistry of Nickel*, Vol. 1, Academic Press, New York, 1974, pp. 244–248.
[16] At elevated temperatures **1** is unstable and the reaction is too fast to be monitored by saturation transfer.
[17] NOE was measured between any two adjacent protons in the system and was found to be non-existent (within the experimental limitation). This is not surprising, since the NOE depends on the molecular mass; it is positive (up to 50%) in small molecules and negative (maximum −100%) in large molecules (see D. Neuhaus and M. Williamson, *The Nuclear Overhauser Effect in Structural and Conformational Analysis*, VCH, New York, 1989, pp. 30–31). It may well be that **3** is at the molecular weight range for which the NOE effect is almost unobservable. Also, the dependence of the measured effect is logarithmic with temperature (see text), whereas the NOE dependence on temperature is of a different nature (see D. Neuhaus and M. Williamson, *The Nuclear Overhauser Effect in Structural and Conformational Analysis*, VCH, New York, 1989, pp. 90–91, 158–160).
[18] (a) A. Hassner, R. Maurya, O. Friedman, H.E. Gottlieb, A. Padwa and D. Austin, *J. Org. Chem., 58* (1993) 4539; (b) R. Glazer, S. Cohen, D. Donnell and L. Agranat, *J. Pharm. Sci., 75* (1986) 772.
[19] In the free ligand the chemical shifts of H(2) and H(3) are similar (see Fig. 2). Since both protons are similarly affected by

the Ni in **3a** and **3a'** respectively, H(2) is expected to have a similar chemical shift to H(3') and vice versa.

[20] Actually, this is true for $\Delta\Delta G_f$, but since the entropy of formation of both isomers (**3a** and **3a'**) is expected to be very similar, it is probably true also for $\Delta\Delta H_f$.

[21] Preliminary results for the effect of methoxy substitutions at different positions on the anthracene are found in A. Shazar, *M.Sc. Thesis*, Technion, Haifa, Israel, 1993.

[22] One quaternary carbon is also unobservable in the free ligand, see C.J. Pouchert and J. Behnke, *The Aldrich Library of ^{13}C and ^{1}H FT NMR Spectra*, Vol. 2, Aldrich Chemical Company, 1st edn., 1993, p. 50.

[23] See M.L. Martin, J.J. Delpuech and G.L. Martin, *Practical NMR Spectroscopy*, Heyden, Chichester, UK, 1980, pp. 315–321.